



# Kinetic Study of the Acylation Reaction of Dibutylcarbonyl Chloride and Dibutylamine

Yi-Bo Zhou<sup>1</sup> Rui Zhu<sup>1</sup> Han-Qi Zhou<sup>1</sup> Jun-Hua Li<sup>1</sup> Feng-Fan Liu<sup>1,2\*</sup>

<sup>1</sup>Key Laboratory for Green Pharmaceutical Technologies and Related Equipment of Ministry of Education and Key Laboratory of Pharmaceutical Engineering of Zhejiang Province, Collaborative Innovation Center of Yangtze River Delta Region Green Pharmaceuticals, Zhejiang University of Technology, Hangzhou, People's Republic of China

<sup>2</sup>Zhejiang Governor Triangle Biomedical Industrial Technology Research Park, Huzhou, People's Republic of China

Address for correspondence Feng-Fan Liu, PhD, Collaborative Innovation Center of Yangtze River Delta Region Green Pharmaceuticals, Zhejiang University of Technology, 18 Chaowang Road, Hangzhou 310014, People's Republic of China (e-mail: liufengfan@zjut.edu.cn).

Pharmaceut Fronts 2023;5:e282–e287.

## Abstract

Tetrabutylurea (TBU) is mainly used as a working liquid in the preparation of hydrogen peroxide via the anthraquinone process. It is reported that dibutylamine (A) reacts with dibutylcarbonyl chloride (B) to produce TBU in the presence of triphosgene, which is the decisive step of the reaction. In this study, we aimed to investigate the reaction kinetics of the decisive step to gain more insight into the reaction. The reaction order as well as the pre-exponential factors ( $A$ ) and the activation energies ( $E_a$ ) were determined. The kinetic study suggested that the total order of the reaction is second.  $E_a = 5.4 \times 10^4$  J/mol,  $A = 1.5257 \times 10^7$  L/(mol  $\times$  min), calculated through a second-order kinetics model. The accuracy and applicability of the kinetic model were verified by several experiments, showing that enhancing reaction temperature could shorten the reaction time and increase the conversion rate.

## Keywords

- ▶ tetrabutylurea
- ▶ dibutylamine
- ▶ dibutylcarbonyl chloride
- ▶ kinetics
- ▶ acylation

## Introduction

Urea has a wide range of applications in pharmacology, agriculture, and industry. Urea structural fragments are important dominant backbones in the field of medicinal chemistry. A compound containing an appropriate amount of urea is often associated with multiple biological activities,<sup>1,2</sup> thus, urea fragments, as one of the most commonly used dominant fragments, play a pivotal role in drug design.<sup>3,4</sup>

Ertl et al considered urea as the 14th most common functional group in biologically active molecules mentioned in the medicinal chemistry literature.<sup>5</sup> The formation of H-bonding interactions between a carbonyl hydrogen bond acceptor and up to two hydrogen bond donors (for disubstituted derivatives) allows modulating a pharmacophore's properties and subsequently influences the drug potency

or acceptor–target interactions. Given this significant importance, the incorporation of urea functionality has been employed to modulate drug potency and selectivity, as well as enhance the properties of anticancer, antibacterial, anticonvulsive, anti-human immunodeficiency virus, antidiabetic agents, and other medicinal compounds.<sup>6–8</sup> Then a variety of urea or thiourea-containing compounds have received market approval from regulatory agencies (Food and Drug Administration and European Medicines Agency) for the treatment of various human diseases. These drugs include sorafenib (a kinase inhibitor),<sup>9</sup> flibanserin (used for treating female hypoactive sexual desire disorder),<sup>10</sup> and cariprazine (an antipsychotic drug),<sup>11</sup> as shown in ▶Fig. 1.

The synthesis of urea derivatives has been explored. As shown in ▶Fig. 2, the traditional method involved the toxic step, including the use of phosgene (BTC),<sup>12</sup> *t*-Boc

received

July 30, 2023

accepted

November 1, 2023

article published online

December 4, 2023

DOI <https://doi.org/>

10.1055/s-0043-1777286.

ISSN 2628-5088.

© 2023. The Author(s).

This is an open access article published by Thieme under the terms of the Creative Commons Attribution License, permitting unrestricted use, distribution, and reproduction so long as the original work is properly cited. (<https://creativecommons.org/licenses/by/4.0/>)

Georg Thieme Verlag KG, Rüdigerstraße 14, 70469 Stuttgart, Germany

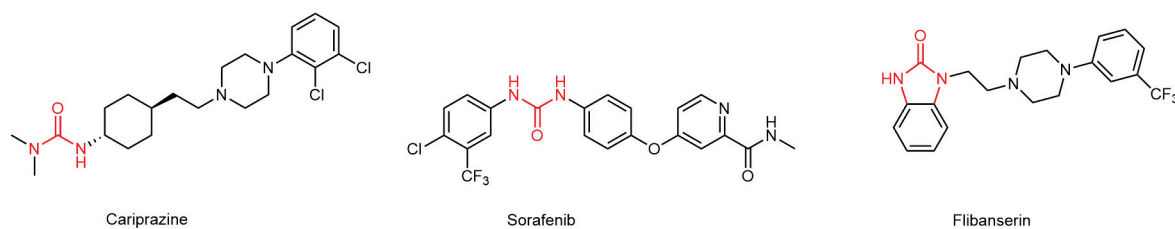


**Fig. 1** Chemical structure of cariprazine, sorafenib, and celioprolool.

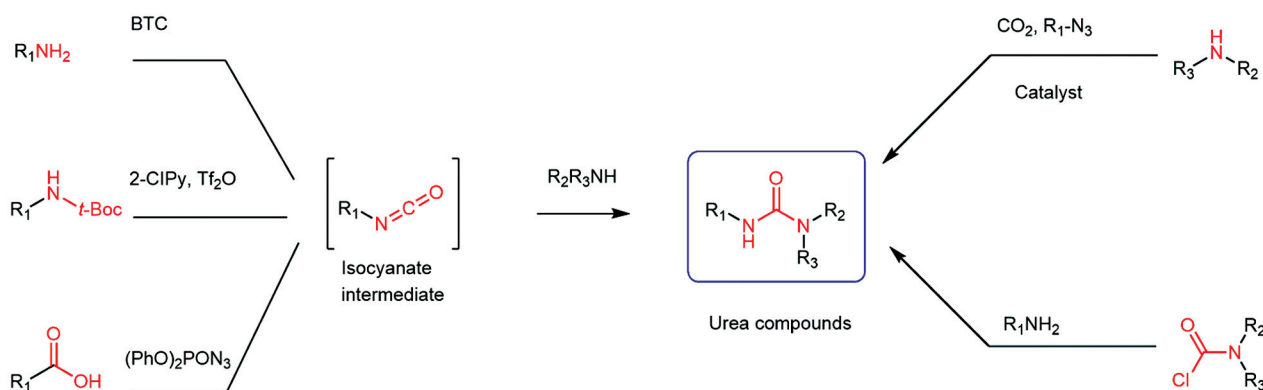


**Fig. 2** Traditional synthesis route of urea compounds.

deprotection reaction,<sup>13</sup> the rearrangement reaction,<sup>14–17</sup> the acylation of carbamoyl chloride and amines,<sup>18,19</sup> as well as the participation of isocyanates. Encouragingly, there are also alternative routes to synthesize urea derivatives, involving the use of less toxic agents like ethylene carbonate or diethyl carbonate, and the direct synthesis of urea derivatives from amines and CO<sub>2</sub> in the presence of numerous catalysts. Interestingly, several ionic liquids were also examined as suitable solvents for the synthesis of the kind of compounds.<sup>20</sup>

Tetrabutylurea (TBU), as a urea derivative, is an extremely versatile intermediate in organic synthesis and used for preparing pesticides, pharmaceuticals, dyes, plastics, plasticizers, and stabilizers, catalysts for photo-gasification reactions, as well as solvents and lubricants. Among those, the most important role of TBU is playing as a solvent to partially or entirely replace trioctyl phosphate in the synthesis of hydrogen peroxide by the anthraquinone process.<sup>21</sup>

TBU is obtained through the reaction of dibutylamine (**A**) with phosgene, biphosgene, or triphosgene in the industry.<sup>22</sup> The route has two steps in turn. First, **A** and triphosgene react quickly to generate the intermediate dibutylcarbamy chloride (**B**). The reaction time is relatively fast and could be ignored. Then, the intermediate **B** reacts with **A**, forming TBU, and this is the decisive step of the reaction. However, its kinetics remains rarely studied. In addition, the conduction of the reaction also faces many problems, such as the adoption of a liquid–liquid heterogeneous system, the mass transfer performance, three waste treatments, and the safe use of phosgene. Therefore, the kinetics of TBU synthesis from **A** and **B** should be investigated to achieve a better understanding of the essential reaction process of TBU.

## Materials and Methods

### Materials

The reagents used in the study were: dibutylamine (**A**, 99.0 wt%, Sinopharm Chemical Reagent Shanghai Co., Ltd.), toluene (analytical grade, Sinopharm Chemical Reagent Shanghai Co., Ltd.), sodium hydroxide (99.0 wt%, Aladdin Industrial Shanghai, China), acetonitrile (analytical grade, Sinopharm Chemical Reagent Shanghai Co., Ltd.), and dibutylcarbamy chloride (**B**, 99.0 wt%, Shanghai Experimental Reagent Co., Ltd.). The reagents were used directly without further purification. A gas chromatograph (GC 9720, Fuli Analytical Instruments Co., Ltd.) equipped with an SE-54 GC column was used for sample analysis.

### Synthetic Route

The synthetic route of TBU is shown in ▶**Fig. 3**; compounds **A** and **B** were heated at 90°C for 6 hours to produce TBU with a yield of 95%. During the process, HCl and **B** formed an amino hydrochloride, which was neutralized in NaOH (aq) to produce NaCl. NaOH (aq) prevents salt formation of HCl and **A** which affects the accuracy of the reaction. Thus, **A** could be dissociated, allowing the reaction to continue. Complex **B**, as the secondary amine, is stable in water and almost no hydrolysis reaction occurs in water.<sup>18</sup>

### Sample Analysis

Collect a small amount of the reaction mixture when the reaction has reached a stable state. After cooling the reaction mixture, the organic layer was separated and diluted 10 times with acetonitrile. With sufficient cooling and dilution, the reaction no longer proceeds. To avoid inaccuracy, the

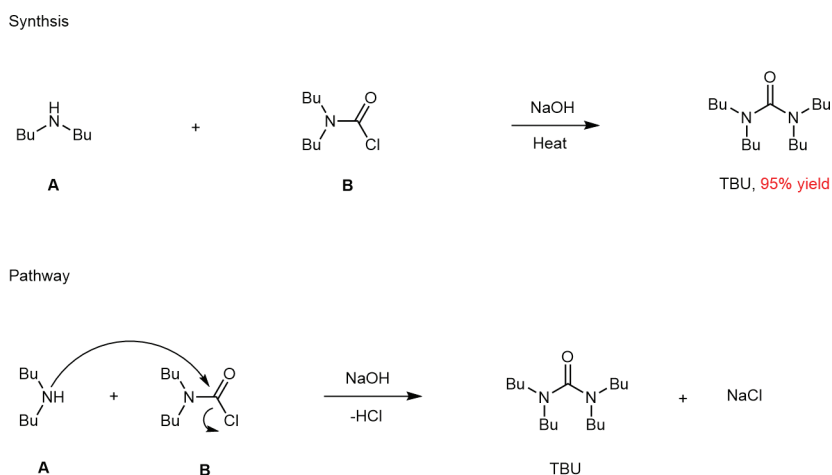


**Fig. 3** Synthesis route of TBU and the pathway of each substance. TBU, tetra-butylurea.

diluted sample is analyzed with GC immediately. The reaction conversion is obtained by an external standard method. Each sample is tested three times to ensure the accuracy of the results.

### Experiment

An intermittent reaction was performed using a magnetic stirring device (MR Hei-Tec, Heidolph) with a heating function. The reaction order of compound **A** was determined as follows: the toluene solution of compound **A** and the NaOH (aq) was heated to reaction temperature in a three-necked flask, and the toluene solution of compound **B** was preheated to the reaction temperature, then poured into the three-necked flask at one time quickly. The whole process was carried out at a stirring speed of 800 rpm, and samples were taken regularly during the reaction period to calculate the conversion rate of the reaction.

The fluctuation range of the reaction temperature was less than 1°C, suggesting an isothermal process of the batch reaction. After sampling, the samples were diluted and cooled to ensure that the reaction did not continue.

## Results and Discussion

### Reaction Route and Mixing Performance Analysis

As shown in ►Fig. 3, acylation was the reaction type and TBU was formed by nucleophilic addition of **A** and **B** under high-temperature conditions. The HCl, produced by the nucleophilic addition of **A** and **B**, forms a dibutylamine hydrochloride with **A** that may influence the proceeding of the reaction. However, with the presence of NaOH (aq), dibutylamine hydrochloride was neutralized to release compound **A**, which nucleophilic attacks the carbonyl carbon of compound **B** to form the target product.

A better mixing between aqueous and organic phases led to a higher reaction efficiency and a lower experimental error. The reaction was carried out in a liquid–liquid two-phase reaction system, thus, an efficient mixing performance was crucial for the study of the intrinsic kinetics of the reaction. ►Fig. 4 demonstrates the conversion rate of **B** at

different speeds with the same residence time. Our data showed that when magnetic stirring speed exceeded 600 rpm, mass transfer effects were considered eliminated, reaching an ideal mixing state controlled only by reaction kinetics.

After the reaction reaches a better mixed state, the kinetic study of the reaction was determined according to Equation (1):

$$\frac{dC_{TBU}}{dt} = k_1 C_A^\alpha C_B^\beta \quad (1)$$

where  $\alpha$  and  $\beta$  represent the reaction order.

### The Reaction Orders

The reaction order of **B** was assessed. The initial concentration of **A** was set to 10 times the initial concentration of **B**, at which point it was considered that the concentration of **A** does not affect the rate of reaction. Therefore, the reaction rate ( $r_1$ ) of the thermal reaction stage was calculated as

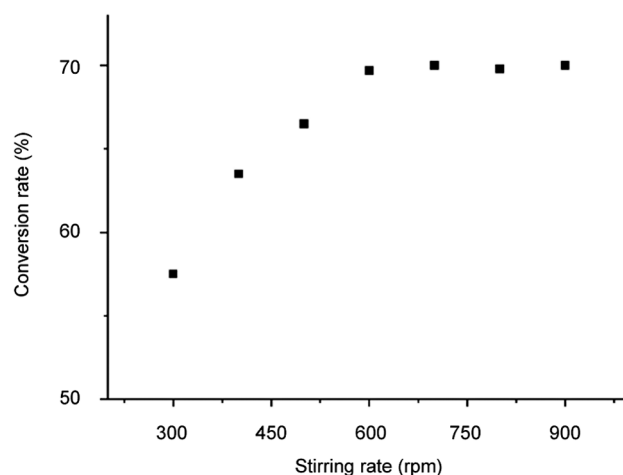


**Fig. 4** Effect of the external diffusion in batch reaction. *Reaction conditions:* 30 mL of solutions **A**, **B**, and NaOH (aq) in 250 mL three-necked flask; initial concentrations of **A**, **B**, and NaOH (aq) in the reaction mixture were 0.5, 0.5, and 0.5 mol/L, respectively; reaction temperature = 80°C; reaction time = 1 hour.

Equation (2). Similarly, when the number of reaction stages of **A** was determined, the reaction rate ( $r_2$ ) was calculated as Equation (3).

$$r_1 = k_1 C_A^\alpha C_B^\beta \approx K_\alpha C_B^\beta \quad (2)$$

$$r_2 = k_1 C_A^\alpha C_B^\beta \approx K_\beta C_A^\alpha \quad (3)$$

If the reaction order of **B** was zero, the integral equation of the rate equation can be written as Equation (4), and the plot of  $C_B$  versus  $t$  should also be a straight line. If the reaction order of **B** was first, the integral equation of the rate equation can be written as Equation (5), and the plot of  $\ln(C_B)$  versus  $t$  should also be a straight line. If the reaction order of **B** was second, the integral equation of the rate equation can be written as Equation (6), and the plot of  $1/C_B$  versus  $t$  should also be a straight line.

$$C_{B0} - C_B = K_\alpha t \quad (4)$$

$$\ln C_{B0} - \ln C_B = K_\alpha t \quad (5)$$

$$\frac{1}{C_B} - \frac{1}{C_{B0}} = K_\alpha t \quad (6)$$

where  $C_{B0}$  is the initial concentration of **B** and  $C_B$  is the concentration of **B** at different times.  $C_{A0}$  is the initial concentration of **A** and  $C_A$  is the concentration of **A** at different times. Similarly, the reaction order ( $\alpha$ ) of **A** is found in the same way as  $\beta$ .

To avoid a mistaken judgment caused by the short sampling range, the experiment was preferred in a batch reaction at a low concentration and low temperature, thus, the conversion rates could be determined continuously and conveniently until the conversion rates reached about 90%. The reaction order was an intrinsic property, irrelevant to the reaction mode.

A plot of  $\ln(C_B)$  and  $t$  is shown in ►Fig. 5; compound **B** obtained the highest linear correlation coefficient in the first-

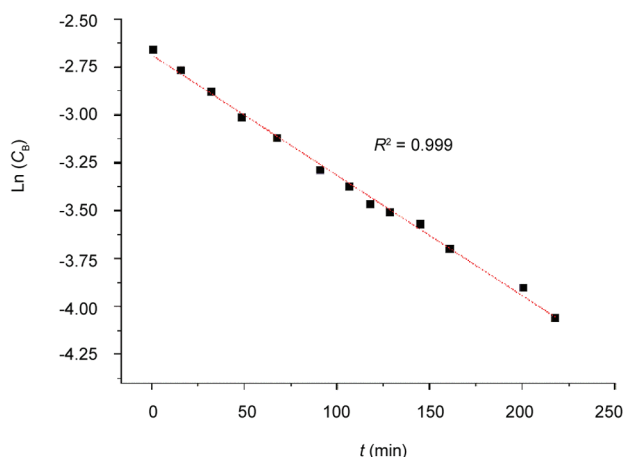


**Fig. 5** Kinetic fitting curves under each reaction order of **B**. Reaction conditions: initial concentration of **A**, **B**, and NaOH (aq) in the reaction mixture was 0.7, 0.07, and 0.07 mol/L respectively; reaction temperature = 70°C; stirring rate = 800 rpm.

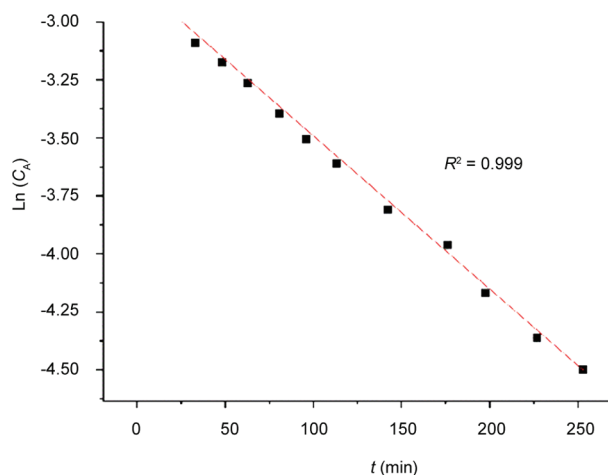


**Fig. 6** Kinetic fitting curves under each reaction order of **A**.

Reaction conditions: initial concentration of **A**, **B**, and NaOH (aq) in the reaction mixture was 0.07, 0.7, and 0.07 mol/L respectively; reaction temperature = 70°C; stirring rate = 800 rpm.

order kinetic fit model ( $R^2 = 0.999$ ); however, an obvious deviation was observed between the data and the fitting line in the zero and second order of **B** ( $R^2 = 0.938$  and  $0.963$ , respectively). The kinetic model of first-order concerning **B** concentration seemed more suitable to represent the reaction, thus  $\beta = 1$ .

A plot of  $\ln(C_A)$  and  $t$  is shown in ►Fig. 6; compound **A** also obtained the highest linear correlation coefficient in the first-order kinetic fit model ( $R^2 = 0.999$ ); however, a bad correlation level between the zero and second order of **B** ( $R^2 = 0.933$  and  $0.965$ ) was observed. The kinetic model of first-order concerning **A** concentration seemed more suitable to represent the reaction; therefore,  $\alpha = 1$  should be considered.

The reaction orders for both **A** and **B** were the first order. Therefore, the reaction behaves kinetically as a secondary reaction, and its reaction kinetic equation could be written as Equation (7).

$$\frac{dC_{TBU}}{dt} = k_1 C_A^1 C_B^1 = k_1 C_A C_B \quad (7)$$

As mentioned above, a wide range of the conversion rates is very necessary, if the range of the conversion rates was only from 0 to about 50%, the three fitting parameters of correlation coefficient  $R^2$  were similar, and we may achieve a wrong conclusion.

### Rate Constant ( $k_1$ ), Activation Energy, and Pre-exponential Factor

The kinetic data were collected at different temperatures and residence times and the results are shown in ►Fig. 7A. Our data showed that the trend of the conversion rate of the reaction with time was consistent with the secondary reaction law.

The initial concentrations of **A** and **B** were the same; therefore, the reaction kinetic equation could be written as Equation (8), and its integral equation expressed by the

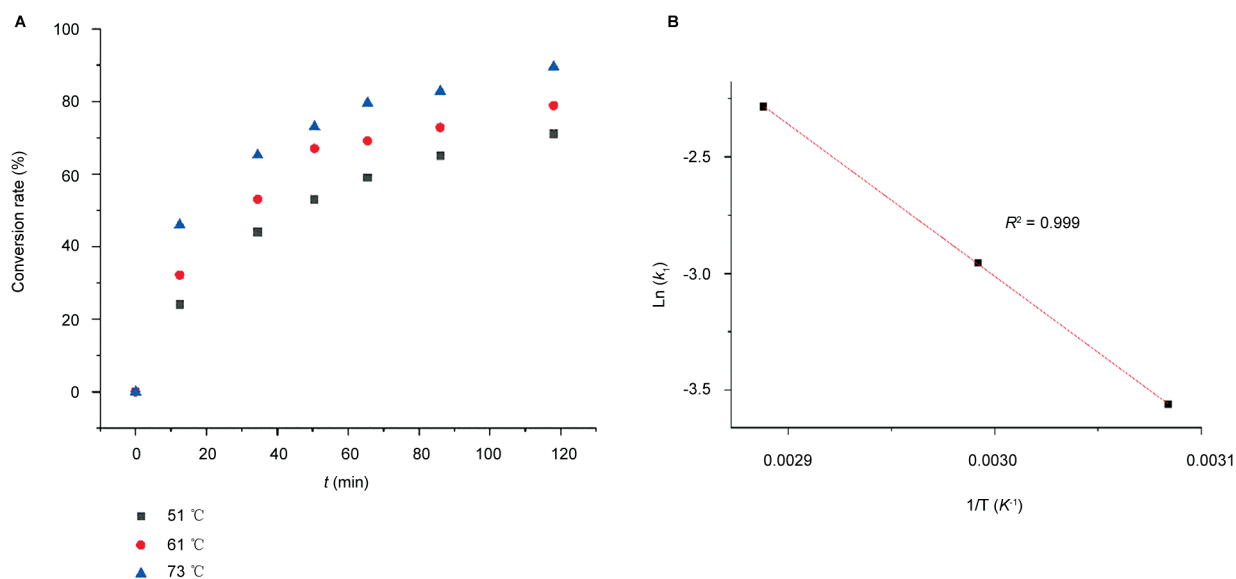


**Fig. 7** (A) Conversion rate of **A** under different temperatures. Reaction conditions: the initial concentration of **A**, **B**, and NaOH (aq) in the reaction mixture was 0.5, 0.5, and 0.5 mol/L, respectively; stirring rate = 800 rpm. (B) The plot of  $\ln(k_1)$  and  $1/T$ .  $T$ , temperature.

conversion rate of **A** ( $x_A$ ) can be expressed as Equation (9),  $k_1 = K/C_{A0} \cdot x_A/(1-x_A)$  had a linear relationship with  $t$ . Values of  $K$  and  $k_1$  at different temperatures can be easily calculated and the results are shown in ►Table 1. According to the Arrhenius equation (Equation 10),  $1/T$  and  $\ln(k_1)$  can be linearly fitted, as shown in ►Fig. 7B.  $E_a$  and  $A$  can be obtained through calculation and the results are shown in ►Table 2. The  $A$  and  $E_a$  values of the reaction between **A** and **B** as we have known were first reported.

$$\frac{dC_A}{dt} = -k_1 C_A^1 C_B^1 = k_1 C_A C_B = k_1 C_A^2 \quad (8)$$

$$\frac{x_A}{1-x_A} = k_1 C_{A0} t = K t \quad (9)$$

$$\ln k_1 = \ln A - \frac{E_a}{RT} \quad (10)$$

### Kinetic Model Validation

Based on the kinetic study, we obtained the kinetic parameters of  $k_1$ ,  $E_a$ , and  $A$ , and the reaction rate expression for

**Table 1** The value of  $k_1$  at different temperatures

$T$ (°C)	$1/T$ (K <sup>-1</sup> )	$k_1$ (L mol <sup>-1</sup> min <sup>-1</sup> )	$\ln k_1$
51	0.003084	0.0284	-3.5620
61	0.002992	0.0521	-2.9551
73	0.002888	0.1018	-2.2843

Abbreviation:  $T$ , temperature.

**Table 2** Values of  $A$  and  $E_a$

Factors	$A$ (L mol <sup>-1</sup> min <sup>-1</sup> )	$E_a$ (J/mol)
Values	$1.5257 \times 10^7$	$5.4 \times 10^4$

Abbreviations:  $A$ , pre-exponential factor;  $E_a$ , activation energy.

the thermal reaction phase could be derived as Equation (11). Therefore, a complete reaction kinetic model was established. To test the accuracy and applicability range (concentration and temperature) of the kinetic model, a series of validation experiments were designed. The concentration range of **A** and **B** was 1.2 to 1.6 mol/L and the reaction temperature was 30 to 90 °C. The reaction time was within 1 hour and the results are shown in ►Table 3. The conversion rate of this reaction increased with the increased temperature and substrate concentration and the deviations between the calculated and experimental values of  $x_A$  were all around 1%, indicating that the kinetic model was valid. Thus, changing the parameters in the applied range in theory, the kinetic model simulation can be used to assess the effect of each reaction parameter on selectivity and an excellent yield could be obtained by calculating the residence time in an optimized condition.

$$t = \frac{1}{C_{A0} \times 1.5257 \times 10^7 e^{-\frac{5.4 \times 10^4}{RT}}} \times \frac{x_A}{1-x_A} \quad (11)$$

### Conclusion

In this work, we have successfully investigated the kinetics of the reaction between dibutylamine and **B** to form TBU. From the results of the kinetic study, the total order of the reaction is second with  $E_a$  being  $5.4 \times 10^4$  J/mol and  $A$  being  $1.5257 \times 10^7$  L mol<sup>-1</sup> min<sup>-1</sup>. From the kinetic study, we derived the reaction rate expression that can serve as a useful guide for optimizing reaction conditions. Validation experiments demonstrated good agreement between our kinetic model and experimental results across a wide range of concentrations and temperatures. The model simulations indicated that increasing the reaction temperature could shorten the reaction time while increasing the conversion rate. Overall, the acylation reaction kinetic model has important implications for synthesizing drugs containing urea structures.

**Table 3** The experimental data and calculated data of  $x_A$  under different conditions

$C_{A0}$ (mol/L)	$T$ (°C)	$t$ (min)	Experimental data (%)	Calculated data (%)	Deviations (%)
1.2	30	60	33.3	33.7	1.2
1.4	60	50	76.7	77.4	0.9
1.6	90	40	93.2	94.0	0.8

Reaction conditions: The initial concentrations of A, B, and NaOH (aq) in the reaction mixture were the same; stirring rate = 800 rpm.

#### Funding

We are grateful to the Zhejiang Provincial Key R&D Project (Grant. No. 2020C03006 & 2019-ZJ-JS-03) for financial support.

#### Conflict of Interest

None declared.

#### References

- 1 Ghosh AK, Kovala S, Osswald HL, et al. Structure-based design of highly potent HIV-1 protease inhibitors containing new tricyclic ring P2-ligands: design, synthesis, biological, and X-ray structural studies. *J Med Chem* 2020;63(09):4867–4879
- 2 Garuti L, Roberti M, Bottegoni G, Ferraro M. Diaryl urea: a privileged structure in anticancer agents. *Curr Med Chem* 2016;23(15):1528–1548
- 3 Ronchetti R, Moroni G, Carotti A, Gioiello A, Camaioni E. Recent advances in urea- and thiourea-containing compounds: focus on innovative approaches in medicinal chemistry and organic synthesis. *RSC Med Chem* 2021;12(07):1046–1064
- 4 Siddiqui N, Alam MS, Stables JP. Synthesis and anticonvulsant properties of 1-(amino-N-arylmethanethio)-3-(1-substituted benzyl-2, 3-dioxindolin-5-yl) urea derivatives. *Eur J Med Chem* 2011;46(06):2236–2242
- 5 Ertl P, Altmann E, McKenna JM. The most common functional groups in bioactive molecules and how their popularity has evolved over time. *J Med Chem* 2020;63(15):8408–8418
- 6 Li HQ, Lv PC, Yan T, Zhu HL. Urea derivatives as anticancer agents. *Anticancer Agents Med Chem* 2009;9(04):471–480
- 7 Batra S, Tusi Z, Madapa S. Medicinal chemistry of ureido derivatives as anti-infectives. *Anti-Cancer Agent Me* 2006;5(02):135–160
- 8 Hodge CN, Aldrich PE, Bachelier LT, et al. Improved cyclic urea inhibitors of the HIV-1 protease: synthesis, potency, resistance profile, human pharmacokinetics and X-ray crystal structure of DMP 450. *Chem Biol* 1996;3(04):301–314
- 9 Wilhelm S, Carter C, Lynch M, et al. Discovery and development of sorafenib: a multikinase inhibitor for treating cancer. *Nat Rev Drug Discov* 2006;5(10):835–844
- 10 Borsini F, Evans K, Jason K, Rohde F, Alexander B, Pollentier S. Pharmacology of flibanserine. *CNS Drug Rev* 2002;8(02):117–142
- 11 Agai-Csogor E, Domány G, Nógrádi K, et al. Discovery of cariprazine (RGH-188): a novel antipsychotic acting on dopamine D3/D2 receptors. *Bioorg Med Chem Lett* 2012;22(10):3437–3440
- 12 Lemoucheux L, Rouden J, Ibazizene M, Sobrio F, Lasne MC. Debenzylation of tertiary amines using phosgene or triphosgene: an efficient and rapid procedure for the preparation of carbamoyl chlorides and unsymmetrical ureas. Application in carbon-11 chemistry. *J Org Chem* 2003;68(19):7289–7297
- 13 Bana P, Lakó A, Kiss NZ. Synthesis of urea derivatives in two sequential continuous-flow reactors. *Org Process Res Dev* 2017;21(04):611–622
- 14 Liu P, Wang Z, Hu X. Highly efficient synthesis of ureas and carbamates from amides by iodosylbenzene-induced hofmann rearrangement. *Eur J Org Chem* 2012;10:1994–2000
- 15 Liang J, Cochran JE, Dorsch WA, et al. Development of a scalable synthesis of an azaindole-pyrimidine inhibitor of influenza virus replication. *Org Process Res Dev* 2016;20(05):965–969
- 16 Narendra N, Chennakrishnareddy G, Sureshbabu VV. Application of carbodiimide mediated Lossen rearrangement for the synthesis of alpha-ureidopeptides and peptidyl ureas employing N-urethane alpha-amino/peptidyl hydroxamic acids. *Org Biomol Chem* 2009;7(17):3520–3526
- 17 Wang CH, Hsieh TH, Lin CC, et al. One-Pot synthesis of N-mono-substituted ureas from nitriles via tiemann rearrangement. *Synlett* 2015;26(13):1823–1826
- 18 Nishizawa A, Takahira T, Yasui K, et al. Nickel-catalyzed decarboxylation of aryl carbamates for converting phenols into aromatic amines. *J Am Chem Soc* 2019;141(18):7261–7265
- 19 Singh DV, Adeppa K, Misra K. Mechanism of isoproturon resistance in Phalaris minor: in silico design, synthesis and testing of some novel herbicides for regaining sensitivity. *J Mol Model* 2012;18(04):1431–1445
- 20 Wu CY, Cheng HY, Liu RX, et al. Synthesis of urea derivatives from amines and CO<sub>2</sub> in the absence of catalyst and solvent. *Green Chem* 2010;12:1811–1816
- 21 Ma HQ, Shen C, Feng B, et al. Research progress in synthesis of tetrabutylurea and its application in production of hydrogen peroxide. *Chem Propell Polym Mater* 2021;19(04):26–31
- 22 Ma HQ, Ma YH, Zhao XD, et al. The invention relates to a method for preparing tetrabutylurea by aqueous phase method. CN Patent 108329238B. October, 2020